Stimulated Brillouin Scattering in Multilayer Silicon Nitride Waveguides

Roel Botter
Nonlinear Nanophotonics
University of Twente
Enschede, the Netherlands
r.a.botter@utwente.nl

Radius Suryadharma
Nonlinear Nanophotonics
University of Twente
Enschede, the Netherlands
r.n.setyosuryadharma@utwente.nl

Yvan Klaver
Nonlinear Nanophotonics
University of Twente
Enschede, the Netherlands
y.klaver@utwente.nl

Okky Daulay
Nonlinear Nanophotonics
University of Twente
Enschede, the Netherlands
o.f.p.daulay@utwente.nl

Peter van der Slot
Nonlinear Nanophotonics
University of Twente
Enschede, the Netherlands
p.j.m.vanderslot@utwente.nl

Edwin Klein
LioniX International
Enschede, the Netherlands
e.j.klein@lionix-int.com

Marcel Hoekman
LioniX International
Enschede, the Netherlands
m.hoekman@lionix-int.com

David Marpaung
Nonlinear Nanophotonics
University of Twente
Enschede, the Netherlands
david.marpaung@utwente.nl

2021 International Topical Meeting on Microwave Photonics (MWP) | 978-1-6654-2610-7/21/$31.00 ©2021 IEEE | DOI: 10.1109/MWP53341.2021.9639390

***Abstract*—We investigated stimulated Brillouin scattering (SBS) in two different multilayer silicon nitride waveguides. We report the first observation of SBS in multilayer silicon nitride waveguides. The gain coefficient measured is 0.16 $m^{-1}W^{-1}$ in one of our samples, but SBS gain is absent in the other sample. We developed a simulation method, which shows how the bigger intermediate layer of 500 nm results in high gain, and the smaller layer of 100 nm results in lower gain. We can use these simulations to optimize our waveguide design. This will allow us to functionalize SBS in silicon nitride waveguides.**

***Index Terms*—integrated photonics, nonlinear optics, stimulated Brillouin scattering**

I. Introduction

Stimulated Brillouin scattering (SBS) is a nonlinear optical interaction, where two counter-propagating light waves (a probe and a stronger pump) interfere. This interference generates an acoustic wave through electrostriction. This acoustic wave then generates a grating via the photoelastic effect, resulting in a moving grating. Pump light that scatters of this moving grating undergoes a Doppler shift, which makes it match the probe frequency. This leads to a narrow-band amplification, which has proven useful in creating for example narrow-band filters and sensors [1]. A schematic overview of this process can be seen in Fig. 1.

SBS has proven to be useful in microwave photonics [2], to build filters [3], [4], time delay [5], instantaneous frequency measurements [6] and narrow-band lasers [7].

The gain observed in an SBS interaction is determined by:

$$G = e^{g_0 L_{eff} P_{pump}}, \tag{1}$$

where g_0 is the Brillouin gain coefficient, a property of the waveguide, L_{eff} is the effective length, and P_{pump} is the pump power in the waveguide.

This project was funded by the Nederlandse Organisatie voor Wetenschappelijk Onderzoek (NWO), project numbers 15702 and 740.018.021.

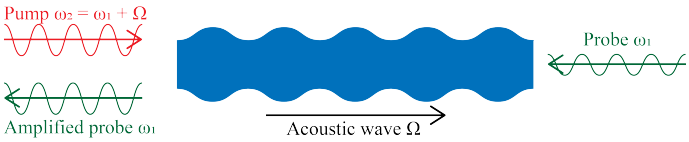

Fig. 1: Schematic overview of SBS.

SBS has previously been observed in low loss single stripe [7], and high confinement thick silicon nitride waveguides [8]. These waveguides have reported gain coefficients of 0.1 and 0.07 $m^{-1}W^{-1}$. However, both of these waveguides have advantages and disadvantages in their use. Single stripe waveguides have low losses, but require large bends, and thick nitride waveguides allow for tight bends, but have a large nonlinear interaction.

Multilayer waveguides, as developed by LioniX have shown promising results for microwave photonics. These waveguides can achieve tight bends, down to 100 µm, combined with low losses, below 0.1 dB/cm [9]. Their first design is called symmetric double stripe (SDS), this is a 1.2 µm wide waveguide that consists of two 170 thick layers of silicon nitride, separated by a 500 nm layer of silicon oxide. At a wavelength of 1550 nm this results in a mode field diameter of 1.6 × 1.7 µm (x × y) and an effective index of 1.535. The waveguide can be coupled to a single-mode fiber by tapering the silicon nitride height to 35 µm. The SDS design was improved to form the asymmetric double stripe (ADS) design. This waveguide is also 1.2 µm wide, but the silicon nitride layers are of different heights, 75 nm for the bottom layer, and 175 nm for the top layer. The intermediate silicon oxide layer has been reduced to 100 nm. This waveguide has a mode field diameter of 1.5 × 1.2 µm (x × y), and the effective index is 1.535, like the SDS. Tapering this waveguide to match a single-mode fiber is achieved by only tapering the top layer to 0 nm, simplifying

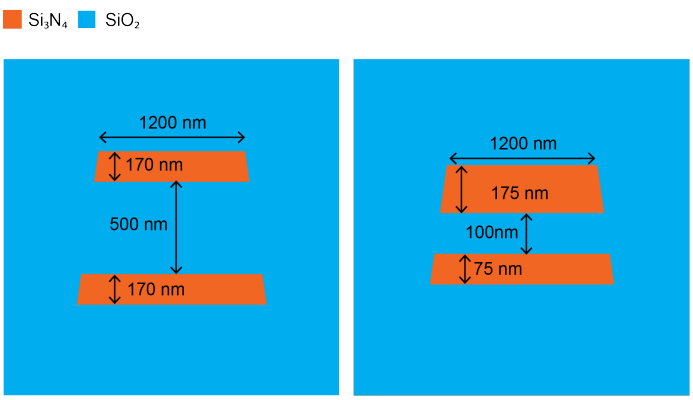

Fig. 2: The geometries we used in our experiment. To the left is the symmetric double stripe (SDS) geometry, and to the right the asymmetric double stripe (ADS) geometry.

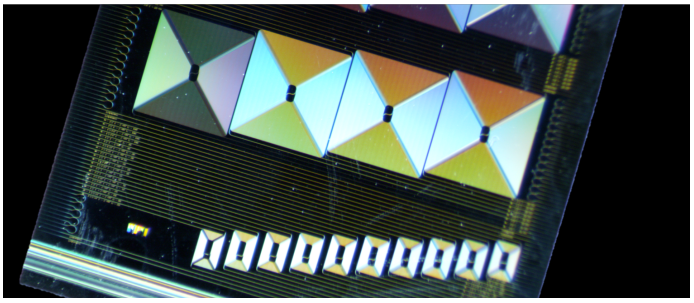

Fig. 3: A photograph our SDS sample, each of the large squares contains two spirals with a length of 50 cm each.

the production process. Both of these geometries can be seen in Fig. 2.

We have previously used these waveguides to create microwave photonic filters [10] and modulation transformers [11]. We aim to enhance this platform by activating SBS, accessing its many applications in signal processing.

II. Experiment

A. Samples

Our samples are 50 cm long spirals of both SDS and ADS waveguides, Fig 3 shows a photograph of the SDS sample. These waveguides are tapered to match standard SMF fiber at the chip edge, resulting in a coupling loss of 1.5 dB per facet. Our SDS and ADS waveguides have optical propagation losses of 0.22 and 0.15 dB/cm respectively.

B. Setup

SBS is weak in silicon nitride, and observing it requires sensitive measurement techniques. Experiments on more Brillouin active waveguides have been performed using a vector network analyzer (VNA) [12]. These techniques utilize a VNA combined with single side modulation to sweep the probe frequency and measure the SBS frequency response. However, trying to measure SBS in our waveguides yielded no results, as the effect is to weak. In our experiment we

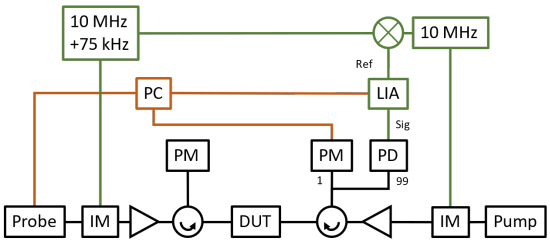

Fig. 4: The setup used in our experiment. DUT: device under test, IM: intensity modulator, LIA: lock-in amplifier, PC: computer, PD: photodiode, PM: power meter.

used the double intensity modulation technique, which has previously been used in Brillouin spectroscopy [13], and later adapted for the detection of stimulated Brillouin scattering in silicon nitride [8]. This technique includes the modulation of both the pump and probe, at slightly different frequencies (10 MHz and 10 MHz + 75 kHz respectively). Any signal that results from the interaction of the two sources (i.e. SBS) will therefore appear at the difference frequency (75 kHz), whereas all signals coming from either the pump or the probe will appear at their respective modulation frequencies. This allows us to use a lock-in amplifier to filter the signal in the electrical domain, rather than use optical filtering techniques. We scan the probe laser to change the pump-probe detuning, and create a frequency response. A schematic overview of our measurement setup can be seen in Fig. 4.

C. Results

Fig. 5 shows the SBS gain curve measured on the SDS sample. The larger peak at 10.9 GHz is a result of the fibers leading up to the chip also exhibiting an SBS interaction. These fibers are 3.5 m in length, and have an SBS gain coefficient of 0.14 $\mathrm{m^{-1}W^{-1}}$ [14]. The smaller peak at 12.75 GHz however, is the SBS peak coming from the sample. This peak is not visible when the chip is not present. We can use the fiber SBS response as a reference point to calculate the chip gain coefficient. By using (1), and taking the small signal approximation we can calculate the gain coefficient using:

$$g_{0,SDS} = \frac{V_{SDS}}{V_{fiber}} \frac{g_{0,fiber} L_{eff,fiber} P_{pump,fiber}}{L_{eff,SDS} P_{pump,SDS}}. \quad (2)$$

Here V denotes the signal amplitude measured by the lock-in amplifier, the subscripts *fiber* and *SDS* refer to the properties of the fiber and chip used in this experiment. This results in a gain coefficient of 0.16 $\mathrm{m^{-1}W^{-1}}$, which is higher than that seen in previous works using silicon nitride [7], [8].

However, when we measure the SBS gain curve using the ADS sample, we only see the fiber peak, as shown in Fig. 6. This suggests that the signal coming from the chip is too low to be measured in our setup.

III. Simulations

We want to know what causes the large discrepancy between our samples, therefore we developed an SBS simulation

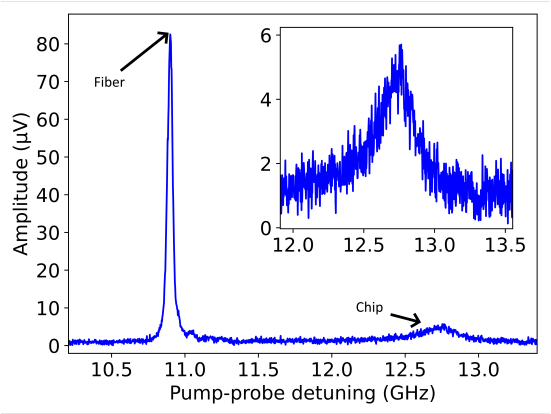

Fig. 5: The experimental result for the SDS sample. The peak at 10.9 GHz is due to the fiber pigtail. The peak at 12.75 GHz is the chip SBS response. Inset: enhanced view of the chip SBS peak.

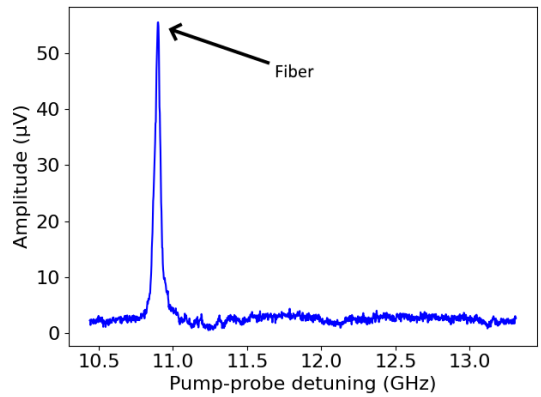

Fig. 6: The experimental result, for the ADS sample. The only peak observed here is from the fiber pigtail.

method in COMSOL to further understand their responses. The simulation starts with the calculation of the optical mode, using a 2D Mode analysis. The optical mode is then used to calculate the electrostrictive force on the waveguides. By varying the frequency at which this force oscillates, we can emulate a scan of the pump-probe detuning. We then use a 2D solid mechanical solver to calculate the acoustic response of the waveguide when subjected to this driving force. The SBS gain is then calculated via the overlap integral between the optical force and the acoustic velocity [15].

We compared our simulation and experiment for the SDS waveguide in Fig. 7. This graph shows good agreement between our simulation and experiment. The shape and width of the two curves match, and the simulation shows smaller peaks on the lower slope of the SBS response, between 12.4 and 12.6 GHz, indicating multiple acoustic modes, which explains the asymmetry of the response peak.

To compare the SDS and ADS waveguides, we look at the optical modes for both waveguides (Fig. 8(a) and 9(a) for SDS and ADS respectively), as well as the acoustic response at

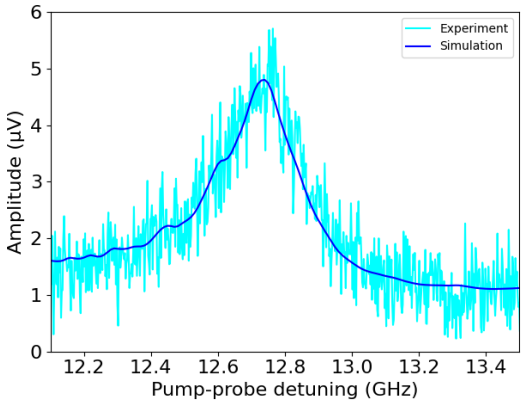

Fig. 7: The simulation result compared to our experimental result. In the small signal approximation the gain coefficient in $m^{-1}W^{-1}$ is linear to the measured signal in μV. The two curves have been scaled to match.

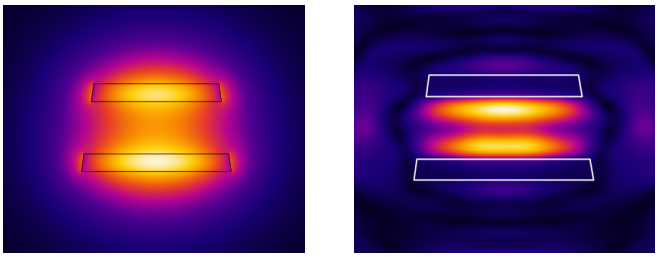

(a) (b)

Fig. 8: The fields found in the SDS simulation: (a) the electrical field of the optical mode, and (b) the displacement of the peak SBS gain frequency.

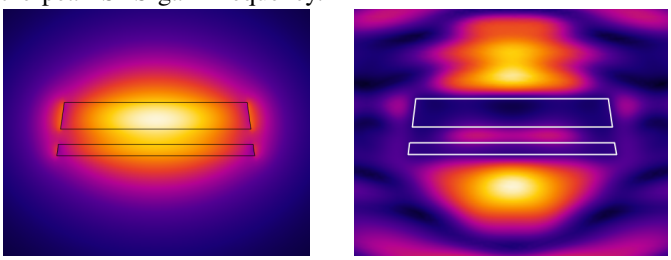

(a) (b)

Fig. 9: The fields found in the ADS simulation: (a) the electrical field of the optical mode, and (b) the displacement of the peak SBS gain frequency.

the frequency of the SDS gain peak (Fig. 8(b) and 9(b) for SDS and ADS respectively. When doing so large differences in the acoustic response can be observed. The acoustics in the SDS are mainly in the intermediate layer, whereas in the ADS the acoustics are outside of the waveguide. This has two effects, one, the overlap between the optics and the acoustics is much higher in the SDS, and two, the SDS shows acoustic guidance between the silicon nitride layers. We believe that this explains the drastically reduced interaction in the ADS waveguide compared to the SDS.

IV. Conclusion

We have observed the first signature SBS in multilayer silicon nitride waveguides. The SBS interaction in the SDS sample is higher than that reported in earlier works involving silicon nitride. The gain coefficient is estimated at around 0.16 $m^{-1}W^{-1}$, and the shift is 12.75 GHz.

We have also the marked difference of the SDS and ADS samples. Altough the waveguides are optically very similar, their SBS response is very different. This shows us that the SDS waveguide is a good starting point for the creation of a waveguide with a higher SBS interaction, and the ADS waveguide is more suitable for applications that require SBS suppression. We have developed a simulation framework, which gives us insight into the differences between our geometries. We are using these simulation tools to optimize our geometries, so we can build waveguides that we can use to functionalize SBS.

References

[1] B. J. Eggleton, C. G. Poulton, P. T. Rakich, M. J. Steel, and G. Bahl, "Brillouin integrated photonics," *Nature Photonics*, 2019.

[2] D. Marpaung, J. Yao, and J. Capmany, "Integrated microwave photonics," *Nature Photonics*, vol. 13, no. 2, pp. 80–90, 2019.

[3] A. Zadok, A. Eyal, and M. Tur, "Gigahertz-wide optically reconfigurable filters using stimulated Brillouin scattering," *Journal of Lightwave Technology*, vol. 25, no. 8, pp. 2168–2174, 2007.

[4] W. Wei, L. Yi, Y. Zhang, Y. Jaouen, Y. Song, Y. Dong, and W. Hu, "A bandwidth-tunable narrowband rectangular optical filter based on stimulated brillouin scattering," *Optics InfoBase Conference Papers*, vol. 22, no. 19, pp. 2168–2174, 2014.

[5] I. Aryanfar, D. Marpaung, A. Choudhary, Y. Liu, K. Vu, D.-Y. Choi, P. Ma, S. Madden, and B. J. Eggleton, "Chip-based Brillouin radio frequency photonic phase shifter and wideband time delay," *Optics Letters*, vol. 42, no. 7, p. 1313, 2017.

[6] W. Zou, X. Long, X. Li, G. Xin, and J. Chen, "Brillouin instantaneous frequency measurement with an arbitrary response for potential real-time implementation," *Optics Letters*, vol. 44, no. 8, p. 2045, 2019.

[7] S. Gundavarapu, G. M. Brodnik, M. Puckett, T. Huffman, D. Bose, R. Behunin, J. Wu, T. Qiu, C. Pinho, N. Chauhan, J. Nohava, P. T. Rakich, K. D. Nelson, M. Salit, and D. J. Blumenthal, "Sub-hertz fundamental linewidth photonic integrated Brillouin laser," *Nature Photonics*, vol. 13, 2018.

[8] F. Gyger, J. Liu, F. Yang, J. He, A. S. Raja, R. N. Wang, S. A. Bhave, T. J. Kippenberg, and L. Thévenaz, "Observation of Stimulated Brillouin Scattering in Silicon Nitride Integrated Waveguides," *Physical Review Letters*, vol. 124, no. 1, 2020.

[9] C. G. H. Roeloffzen, P. W. L. van Dijk, L. Zhuang, R. G. Heideman, R. M. Oldenbeuving, C. Taballione, L. S. Wevers, M. Benelajla, M. Hoekman, Y. Fan, D. Marchenko, J. P. Epping, K.-J. Boller, R. Dekker, A. van Rees, K. Worhoff, R. B. Timens, D. Marpaung, Y. Liu, C. Taddei, E. J. Klein, R. Grootjans, D. Geuzebroek, A. Alippi, A. Leinse, I. Visscher, E. Schreuder, and D. Geskus, "Low-Loss Si3N4 TriPleX Optical Waveguides: Technology and Applications Overview," *IEEE Journal of Selected Topics in Quantum Electronics*, vol. 24, no. 4, pp. 1–21, 2018.

[10] O. Daulay, R. Botter, and D. Marpaung, "On-chip programmable microwave photonic filter with an integrated optical carrier processor," *OSA Continuum*, vol. 3, no. 8, p. 2166, 2020.

[11] O. Daulay, G. Liu, and D. Marpaung, "Microwave photonic notch filter with integrated phase-to-intensity modulation transformation and optical carrier suppression," *Optics Letters*, vol. 46, no. 3, pp. 488–491, 2021.

[12] D. Marpaung, B. Morrison, M. Pagani, R. Pant, D.-Y. Choi, B. Luther-Davies, S. J. Madden, and B. J. Eggleton, "Low-power, chip-based stimulated Brillouin scattering microwave photonic filter with ultrahigh selectivity," *Optica*, vol. 2, no. 2, p. 76, 2015.

[13] W. T. Grubbs and R. A. MacPhail, "High resolution stimulated Brillouin gain spectrometer," *Review of Scientific Instruments*, vol. 65, no. 1, pp. 34–41, 1994.

[14] A. Kobyakov, M. Sauer, and D. Chowdhury, "Stimulated Brillouin scattering in optical fibers," *Advances in Optics and Photonics*, vol. 2, no. 1, pp. 1–59, 2010.

[15] P. T. Rakich, C. Reinke, R. Camacho, P. Davids, and Z. Wang, "Giant enhancement of stimulated Brillouin scattering in the subwavelength limit," *Physical Review X*, vol. 2, p. 011008, 2012.